

Physics 221A: (a) Phase diffusion, phase dynamics (b) Fixed-flux convection

Robin Heinonen (Lectures by P.H. Diamond)

June 6, 2017

1 Introduction

So far, we have used the envelope formalism to investigate pattern formation in nonlinear systems. Using the assumptions of near marginal stability and minimal symmetry we have derived the possible pattern base states, and then determined secondary roughening or “textures” on those base states. This procedure utilizes linear instability theory. For example, the equation

$$\gamma\tau_0 = (\text{Ra} - \text{Ra}_{crit}) - \epsilon_0^2(q - q_0)^2 \quad (1)$$

was used to model the base state near marginality in Rayleigh-Bénard convection, which were roughened by the Eckhaus and zigzag instabilities.

In this chapter, we seek a “deeper” formalism. Recall the phase-winding solution to the Newell-Whitehead equation: the dynamics were governed by the equations

$$\partial_t\phi = \frac{\epsilon_0^2}{\tau_0} \left(\partial_x^2\phi + \frac{2\partial_x|A|\partial_x\phi}{|A|} \right) \quad (2)$$

$$\tau_0\partial_t|A| = (r - \epsilon_0^2(\partial_x\phi)^2)|A| + \epsilon_0^2\partial_x^2|A| - g_0|A|^3 \quad (3)$$

and using $\phi = \delta kx + \tilde{\phi}$, we observe that setting $\epsilon_0^2\delta k^2 \sim r$ eliminates the amplitude growth. Moreover (from Eq. 2), the phase evolves *diffusively* and, at large length scales, *slowly*. In particular, the amplitude is effectively slaved to phase; the formation of textures is rooted in the phase evolution.

Our approach, then, will be to examine pattern formation by applying slowly varying perturbations in phase and exploiting ordering at long wavelengths. This approach goes beyond linear perturbation theory, which was used to derive the Eckhaus and zigzag instabilities.

2 Phase diffusion formalism

This leads us to the phase diffusion formalism introduced by Pomeau and Manneville (1979) [2], a sort of nonlinear eikonal theory approach. The key idea will be to replace invariance

under a uniform phase shift with *approximate* invariance under a *weakly-varying* phase shift to exploit long wavelength ordering.

We seek to characterizing pattern formation by determining effective (not necessarily positive) phase diffusion coefficients D_{\parallel} and D_{\perp} so that

$$\partial_t \phi = D_{\parallel} \partial_x^2 \phi + D_{\perp} \partial_y^2 \phi + \text{h.o.t.} \quad (4)$$

In particular, $D_{\parallel} < 0$ leads to the Eckhaus instability and $D_{\perp} < 0$ leads to the zigzag instability.

Let us proceed by considering the Swift-Hohenberg model

$$\partial_t W = rW - (\partial_x^2 + q_0^2)^2 W - W^3, \quad (5)$$

where $r = \text{Ra} - \text{Ra}_{crit}$ is the distance to threshold and q_0 is the marginal wavevector; take $r > 0$. Fourier transforming Eq. 5 in space and linearizing, we obtain

$$\partial_t W = (r - (k^2 - q_0^2)^2) W \quad (6)$$

and, assuming r is small, we see that the marginal solution is unstable against perturbations with wavevector $k = q_0 + \delta k$, where $|\delta k| < \sqrt{r}/2q_0$.

For the remainder of this discussion, let us set q_0 to unity. Demanding $\delta_t W = 0$, one finds that Eq. 5 has the periodic stationary solution

$$W_0(x) = W^{(1)} \sin(x) + W^{(3)} \sin(3x) + \mathcal{O}(r^2), \quad (7)$$

where $W^{(1)} = \sqrt{\frac{4}{3}(r - 4\delta k^2)}$ and $W^{(3)} = (W^{(1)})^3/256$.

This is the base state. We first make the uniform translation $W_0(x) \rightarrow W_0(x + \phi)$. Expanding, we have

$$W_0(x + \phi) = W_0(x) + \phi \partial_x W_0 + \frac{1}{2} \phi^2 \partial_x^2 W_0 + \dots \quad (8)$$

For ease of notation let \mathcal{F} be the Swift-Hohenberg operator

$$\mathcal{F}(W_0) \equiv rW_0 - (\partial_x^2 + 1)^2 W_0 - W_0^3 \quad (9)$$

and let

$$\Lambda_0 \equiv \left. \frac{\delta \mathcal{F}}{\delta W} \right|_{W_0} = r - (\partial_x^2 + 1)^2 - 3W_0^2. \quad (10)$$

Eq. 5 is translation invariant, so we Taylor expand \mathcal{F} and demand the stationary Swift-Hohenberg equation be satisfied, i.e.

$$\partial_t (W_0(x) + \phi \partial_x W_0 + \dots) = 0 = \mathcal{F}(W_0 + \phi \partial_x W_0 + \dots) = \mathcal{F}(W_0) + \Lambda_0(\phi \partial_x W_0) + \dots \quad (11)$$

By definition, $\mathcal{F}(W_0) = 0$, so it follows that

$$\partial_x \mathcal{F}(W_0) = 0 = \frac{\delta \mathcal{F}}{\delta W} (\partial_x W_0) = \Lambda_0(\partial_x W_0) \quad (12)$$

and hence $\partial_x W_0$ is a translation mode of Λ_0 with eigenvalue 0, belonging to the kernel of Λ_0 . (Recall that the kernel of Λ_0 is the set of sufficiently smooth functions annihilated by Λ_0 —that is,

$$\ker \Lambda_0 = \{f \in \mathcal{C}^4 : \Lambda_0(f) = 0\}.)$$

Using Eq. 10, $\mathcal{F}(W_0) = 0$, and the fact that ϕ is uniform, we have

$$\partial_t \phi \partial_x W_0 = \phi \Lambda_0(\partial_x W_0) = 0, \quad (13)$$

and we see that the uniform phase must not evolve in time.

We now repeat the above, but allow the phase to vary slowly in space and time: we take $\phi = \phi(x, y, t)$. The spatial dependence will accommodate phase clustering. $W_0(x + \phi)$ is no longer an exact solution to Eq. 5, but the error is small and approaches zero for small $\partial_x \phi$, which is to say at long wavelengths.

Let us then look for solutions of the form

$$W(x, y, t) = W_0(x) + \phi(x, y, t) \partial_x W_0(x) + W_1(x, y, t) + W_2(x, y, t), \quad (14)$$

where W_1 and W_2 are small (at long wavelengths) corrections. We first determine W_1 . We have to first order

$$\partial_t (W_0 + \phi \partial_x W_0 + W_1) = \partial_t \phi \partial_x W_0 = \mathcal{F}(W_0) + \Lambda_0(\phi \partial_x W_0 + W_1), \quad (15)$$

whence one finds after some algebra (carefully noting that Λ_0 now acts on both ϕ and $\partial_x W_0$) that

$$\Lambda_0 W_1 = \partial_t \phi \partial_x W_0 + g(x) \partial_x \phi, \quad (16)$$

where

$$g(x) = 4 (\partial_x^2 + 1) \partial_x^2 W_0. \quad (17)$$

We want to find W_1 satisfying Eq. 16. However, such a solution is not guaranteed to exist. We apply a solvability criterion known as the Fredholm alternative, named for Swedish mathematician Erik Ivar Fredholm. Informally:

Theorem 1 (Fredholm alternative) *Let L be a linear differential operator. Given a function f , consider the equation*

$$Lu = f. \quad (*)$$

Then there exists a solution u to () if and only if $f \in (\ker L^\dagger)^\perp$, which is to say $\langle f|v \rangle = 0$ for all v such that $L^\dagger v = 0$.*

Here, we use the bra-ket notation for the inner product. In this case, Λ_0 is self-adjoint so $\Lambda_0^\dagger = \Lambda_0$. We already determined that $\partial_x W_0$ is in the kernel of Λ_0 , so, invoking the Fredholm alternative, we must have

$$\langle \partial_x W_0 | \partial_t \phi \partial_x W_0 \rangle = 0 \quad (18)$$

leading to the trivial lowest-order equation

$$\partial_t \phi = 0. \quad (19)$$

We cannot treat $\phi \partial_x W_0$ as fast-varying only. To make progress, make explicit the dependence of W_1 on $\partial_x \phi$ and set

$$W_1 = W_1^{(0)} + \partial_x \phi \tilde{W}_1(x); \quad (20)$$

here $\tilde{W}_1(x)$ encodes the slow variation in W . Plugging into Eq. 16, we find

$$\Lambda_0(\tilde{W}_1) = g(x), \quad (21)$$

which can be solved to find \tilde{W}_1 . We now can continue to second order (in general, we could continue to arbitrary order in $\partial_x \phi$) in the phase slope, and via a similar approach for W_2 we find

$$\Lambda_0 W_2 = \partial_t \phi \partial_x W_0 + \partial_x^2 \phi \left[4(\partial_x^2 + 1) \partial_x \tilde{W}_1 + 2(3\partial_x^2 + 1) \partial_x W_0 \right]. \quad (22)$$

We can now invoke the Fredholm alternative again, and this time we arrive at the phase diffusion equation

$$\partial_t \phi = D_{\parallel} \partial_x^2 \phi + D_{\perp} \partial_y^2 \phi. \quad (23)$$

The effective phase diffusion coefficients are given by

$$D_{\parallel} = \frac{\langle \partial_x W_0 | 4(\partial_x^2 + 1) \partial_x \tilde{W}_1 + 2(3\partial_x^2 + 1) \partial_x W_0 \rangle}{\langle \partial_x W_0 | \partial_x W_0 \rangle} = 4 \left(\frac{r - 12\delta k^2}{r - 4\delta k^2} \right) \quad (24)$$

and

$$D_{\perp} = \frac{\partial_x W_0 | 2(\partial_x^2 + 1) \partial_x W_0 \rangle}{\langle \partial_x W_0 | \partial_x W_0 \rangle} = \delta k - \frac{(r - 4\delta k^2)^2}{1024}. \quad (25)$$

Demanding $D_{\parallel} < 0$ and $D_{\perp} < 0$ gives us the conditions for the Eckhaus and zigzag instabilities, respectively.

We have thus derived classical secondary instabilities via a *nonperturbative, structural* approach based on scalar products and symmetries of exact solutions to the Swift-Hohenberg equation above threshold. This is in contrast to the envelope approach, which used linear perturbation theory. We also obtain a small correction (the first term in the LHS of Eq. 25) to the envelope theory result for the zigzag instability threshold.

3 Nonlinear phase dynamics

We now seek to determine nonlinear terms in the phase evolution equation. The structure of the equation can be determined by first noting that $\partial_t \phi$ should be a function of derivatives of ϕ only (and not the magnitude of ϕ), and then demanding overall invariance under the inversion symmetry

$$\begin{aligned} x &\rightarrow -x \\ y &\rightarrow -y \\ \phi &\rightarrow -\phi, \end{aligned}$$

whence we deduce that the lowest-order terms are

$$\partial_t \phi = D_{\parallel} \partial_x^2 \phi + D_{\perp} \partial_y^2 \phi - K \partial_x^4 \phi + g \partial_x \phi \partial_x^2 \phi + \dots \quad (26)$$

Similar to the Kuramoto-Sivashinsky equation, we take $K > 0$ since D_{\parallel} and D_{\perp} can be negative. We wish to obtain the coupling g . To do so, let us consider the Eckhaus problem and ignore the y -direction. We have

$$\partial_t \phi = D_{\parallel} \partial_x^2 \phi - K \partial_x^4 \phi + g \partial_x \phi \partial_x^2 \phi. \quad (27)$$

Put $\phi = \frac{\delta k}{k} + \tilde{\phi}$. Here $\tilde{\phi}$ represents the phase for a structure with a perturbation $k \rightarrow k + \delta k$. Plugging into Eq. 27, we obtain

$$\partial_t \tilde{\phi} = D_{\parallel} \partial_x^2 \tilde{\phi} - K \partial_x^4 \tilde{\phi} + g \frac{\delta k}{k} \partial_x^2 \tilde{\phi} + g \partial_x \tilde{\phi} \partial_x^2 \tilde{\phi}. \quad (28)$$

Collecting coefficients, we find that

$$D_{\parallel}(k + \delta k) = D_{\parallel}(k) + g \frac{\delta k}{k}. \quad (29)$$

Comparing to the Taylor expansion $D_{\parallel}(k + \delta k) = D_{\parallel}(k) + \delta k \frac{dD_{\parallel}}{dk} + \dots$, we conclude

$$g = k \frac{dD_{\parallel}}{dk}. \quad (30)$$

4 Phase dynamics of convection rolls: eikonal theory of textures

Let us now apply our new method of looking at textures to convection rolls. We seek to describe texturing in convection rolls by determining the bending of isophase lines (contours of constant phase) — in particular, their curvature and dilatation (Fig. 1). We note this approach is similar to eikonal theory.

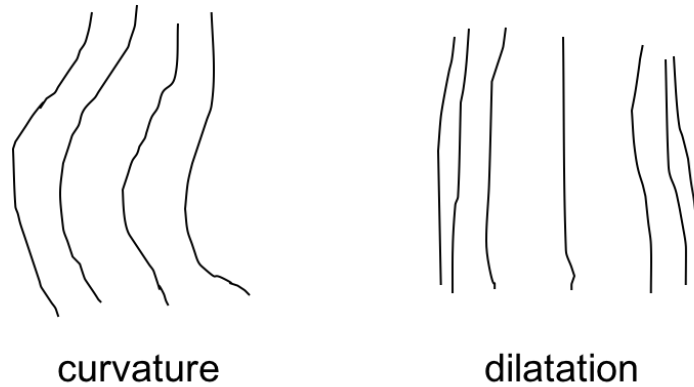


Figure 1: Sketch illustrating curvature and dilatation of sets of isophase lines. Artwork by R. Heinonen

The patterns in the convection rolls are described by level lines in the vertical velocity field $W(x, y, t)$, or equivalently in the velocity field

$$V(x, y, z, t) = V(u(x, y, t), z) \quad (31)$$

where $u = x + \phi(x, y, t)$ is a generalized phase encoding the the horizontal dependence of the velocity field. Note that V_0 is periodic with period $2\pi/k_0$. We naturally wish to assume ϕ is small; however, due to curvature, the phase can accumulate. Instead (again inspired by eikonal theory) it makes sense to track the phase gradient. Thus we seek to describe the pattern by determining $\mathbf{k} = \nabla_h u$ (∇_h refers to a horizontal gradient).

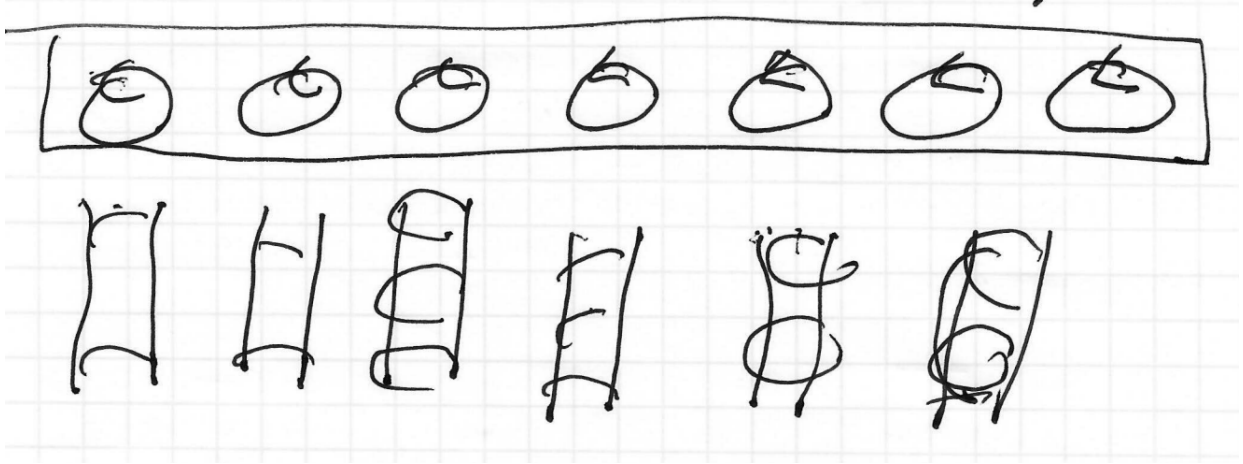


Figure 2: Sketch of convection rolls. The patterns in the rolls are specified by variation in a phase $u(x, y, t)$ which encodes in horizontal dependence of the velocity fields. Artwork by P.H. Diamond

It is useful to define a “director field” (using terminology from liquid crystal physics; see, for example, [3]) $\hat{\mathbf{n}}$ by

$$\mathbf{k} = k\hat{\mathbf{n}}. \quad (32)$$

\mathbf{k} encodes the bending of the isophase lines: we have

$$\nabla_h \cdot \mathbf{k} = \nabla_h(k\hat{\mathbf{n}}) = k\nabla_h \cdot \hat{\mathbf{n}} + \hat{\mathbf{n}} \cdot \nabla_h k; \quad (33)$$

the terms on the RHS represent local curvature and dilatation, respectively.

We now proceed with calculating the phase dynamics. We make the ansatz

$$\frac{\partial u}{\partial t} + v_n \hat{\mathbf{n}} \cdot \nabla u = 0 \quad (34)$$

$$v_n = -D_{\parallel} \hat{\mathbf{n}} \cdot \nabla_h \left(\frac{k}{k_0} \right) - D_{\perp} \nabla_h \cdot \hat{\mathbf{n}}, \quad (35)$$

where v_n is the contour velocity. We check for consistency by plugging Eq. 34 into Eq. 33:

$$\frac{\partial u}{\partial t} - D_{\parallel} \hat{\mathbf{n}} \cdot \nabla_h \left(\frac{k}{k_0} \right) (\hat{\mathbf{n}} \cdot \nabla u) - D_{\perp} \nabla_h \cdot \hat{\mathbf{n}} (\hat{\mathbf{n}} \cdot \nabla u) = 0. \quad (36)$$

Recalling that $u = x + \phi$, we have

$$\partial_x u = 1 + \partial_x \phi = \frac{k_x}{k_0} \quad (37)$$

where k_0 is the wavevector at threshold and so $k/k_0 \simeq 1 + \partial_x \phi$. We then have that $\hat{\mathbf{n}} \cdot \nabla u \simeq 1$ and $\hat{\mathbf{n}} \cdot \nabla(k/k_0) \simeq \partial_x^2 \phi$. Noting additionally that $\nabla \cdot \hat{\mathbf{n}} = \partial_y^2 \phi$, we recover from Eq. 36 the phase diffusion equation

$$\partial_t \phi = D_{\parallel} \partial_x^2 \phi + D_{\perp} \partial_y^2 \phi \quad (38)$$

and so our ansatz was consistent.

We now finally convert the above to a phase dynamics equation à la Cross and Newell (1983) [4]:

$$\tau(k) \partial_t \tilde{u} + \nabla_h \cdot (\mathbf{k} B(k)) = 0, \quad (39)$$

where $\tilde{u} = ku$, and τ and B are a timescale and a phase flux, respectively, to be determined. The phase equation can always be put into this form, which follows by considering the most general rotationally invariant expression that is linear in gradients. We use the definitions to rewrite this as

$$\begin{aligned} 0 &= \tau \partial_t \phi + \nabla_h \cdot (k \hat{\mathbf{n}} B(k)) \\ &= \tau \partial_t \phi + kB(k) \nabla_h \cdot \hat{\mathbf{n}} + \frac{d}{dk} (kB(k)) \hat{\mathbf{n}} \cdot \nabla k \\ &= \tau \partial_t \phi + B(k) \partial_y^2 \phi + \frac{d}{dk} (kB(k)) \partial_x^2 \phi, \end{aligned}$$

valid for almost-parallel rolls. From this we can deduce explicit expansions

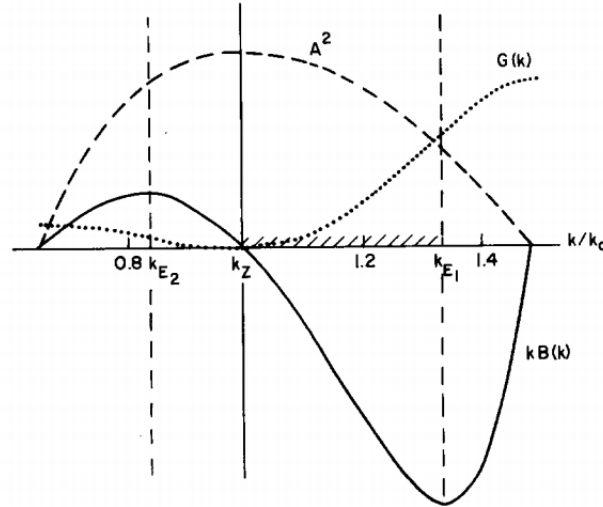


Fig. 2. Typical plot of functions $kB(k)$ (heavy), A^2 (dashed) and $G(k)$ (dotted). Actual plot is for model I with $\nu = 0$ and at $R/R_c = 1.25$. Hatched region of k axis is stability region. Values k_L and k_R denote neutral stability points, k_{E1} , and k_{E2} the Eckhaus instability boundaries and k_z the zig-zag instability boundary.

Figure 3: Typical plot of the flux $kB(k)$ and τ (here A^2). Here $G(k)$ is the negative integral of the flux. Figure “borrowed” from [4]; disregard the inset label of “Fig. 2,” for this is figure 3!

$$D_{\parallel} = -\frac{1}{\tau} \frac{d}{dk} (kB(k)) \quad (40)$$

$$D_{\perp} = -\frac{1}{\tau} B(k). \quad (41)$$

Dividing these equations through, we find

$$\frac{B(k)}{D_{\perp}} = \frac{1}{D_{\parallel}} \left(B(k) + k \frac{dB}{dk} \right) \quad (42)$$

and thus we arrive at an equation for the phase flux B :

$$\frac{dB}{B} = \frac{dk}{k} \left(\frac{D_{\parallel}}{D_{\perp}} - 1 \right). \quad (43)$$

Typical values of the flux $kB(k)$ are presented in Fig. 3. This concludes our discussion of patterns in standard convection.

5 Fixed-flux convection in long, thin systems

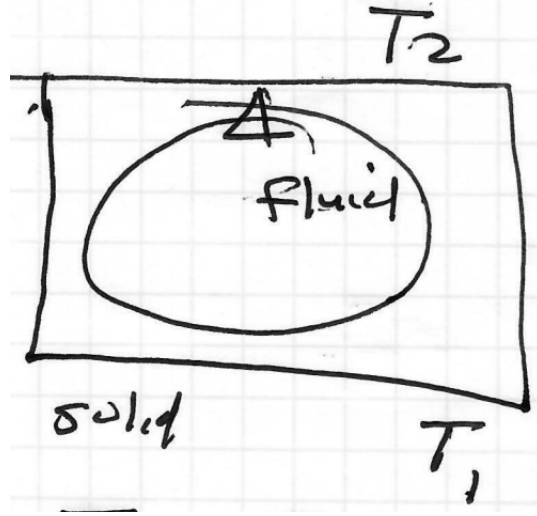


Figure 4: Sketch of the Rayleigh-Bénard convection problem. Artwork by P.H. Diamond

Up until now, we have been considering convection in a system whose boundary plates are at fixed temperature, i.e. they are perfect conductors of heat. This is not necessarily a very physically realistic assumption. More generally, we need only impose the boundary conditions

$$\chi_f \frac{dT_f}{dz} = \chi_s \frac{dT_s}{dz} \quad (44)$$

$$T_f = T_s, \quad (45)$$

where the subscripts s and f refer to the solid plates and fluids, respectively, and χ_{α} is a heat conductivity. Rayleigh-Bénard convection, then, assumes $\chi_s \gg \chi_f$. Let us now study

the opposite limit where the plates are perfect *insulators*. In this case, the heat flux Q and temperature gradient $\frac{dT}{dz}$ are now fixed at the boundaries. Temperature fluctuations in the fluid do not propagate into the solid, so writing $T = T_0 + \theta$, we have

$$\left. \frac{\partial \theta}{\partial z} \right|_{z=0,1} = 0 \quad (46)$$

where $z = 0, 1$ corresponds to the vertical boundaries. We also have that the Nusselt number is equal to unity:

$$\text{Nu} = \frac{Q}{-\chi_f dT/dz} = 1. \quad (47)$$

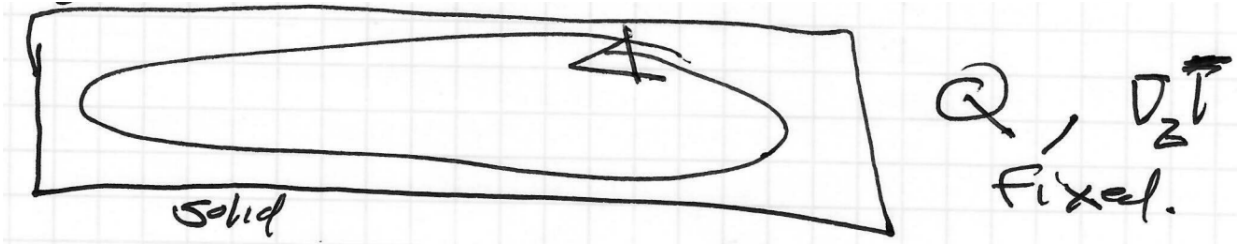


Figure 5: Sketch of the fixed-flux convection problem. Artwork by P.H. Diamond

In Figs. 4 and 5 we compare the two convection problems. For this fixed-flux problem, we restrict ourselves to limit of a long thin box ($L_x \gg L_z$) and strive to determine the structure of patterns in x . We sketch the derivation, originally due to Chapman and Proctor (1980) [5]. We start with the equations of motion [6]

$$\frac{\partial \nabla^2 \phi}{\partial t} - \text{Pr Ra} \frac{\partial \theta}{\partial x} - \text{Pr} \nabla^2 \nabla^2 \phi = \{\nabla^2 \phi, \phi\} \quad (48)$$

$$\frac{\partial \theta}{\partial t} - \frac{\partial \phi}{\partial x} - \nabla^2 \theta = \{\theta, \phi\} \quad (49)$$

where Pr and Ra are the Prandtl and Rayleigh numbers, respectively, ϕ is the stream function (and so $\nabla^2 \phi$ is the vorticity), θ is the normalized temperature, and $\{\cdot, \cdot\}$ refers to the Poisson bracket

$$\{f, g\} = \frac{\partial f}{\partial x} \frac{\partial g}{\partial z} - \frac{\partial g}{\partial x} \frac{\partial f}{\partial z}.$$

We consider slowly-evolving, thin, weakly supercritical cells, and thus introduce a small parameter ϵ and rescale

$$\begin{aligned} x &\rightarrow \epsilon^2 x \\ \phi &\rightarrow \epsilon \phi \\ \partial_t &\rightarrow \epsilon^4 \partial_t \\ \text{Ra} &= \text{Ra}_{crit} + \mu^2 \epsilon^2 \end{aligned}$$

where μ measures the supercriticality of the fluid. Solutions for θ and ϕ are then sought in powers of ϵ :

$$\theta = \theta_0 + \epsilon^2\theta_2 + \epsilon^4\theta_4 + \dots \quad (50)$$

$$\phi = \phi_0 + \epsilon^2\phi_2 + \epsilon^4\phi_4 + \dots \quad (51)$$

At zeroth order one finds solutions of the form $\theta_0 = f(x, t)$ and $\phi = \text{Ra}_{crit} p(z) f'(x, t)$; f is the horizontal cell envelope and $p(z)$ encodes the vertical structure of the cell. The prime indicates a derivative with respect to x . Carrying the calculation to fourth order and applying boundary conditions yields, after some work, the Chapman-Proctor equation for f :

$$\partial_t f + A\mu^2 f'' + Bf'''' + C((f')^3)' + D(f' f'')' = 0. \quad (52)$$

Note that $A > 0$ and $B > 0$ leads to the familiar situation of negative diffusion and positive hyperdiffusion. The Chapman-Proctor equation gives a good description of the horizontal dynamics for slightly supercritical, small-amplitude convection systems. A complete analysis is beyond the scope of these notes, but note that in the case of identical boundary conditions on the plates, symmetry requires $D = 0$ and, defining $g = f'$, we can take the derivative of Eq. 52 to find

$$\partial_t g + A\mu^2 g'' + Bg'''' + C(g^3)'' = 0. \quad (53)$$

This equation can be rescaled to take the form of the so-called Cahn-Hilliard equation [7], which describes the phase separation dynamics of a binary mixture (see appendix). By solving this equation for a stationary state and studying the stability of the nonlinear solutions (which involve elliptic integrals), Chapman and Proctor show that, for a periodic box, the stable flow in the box consists of two flattened, counter-rotating cells (see Fig. 6).

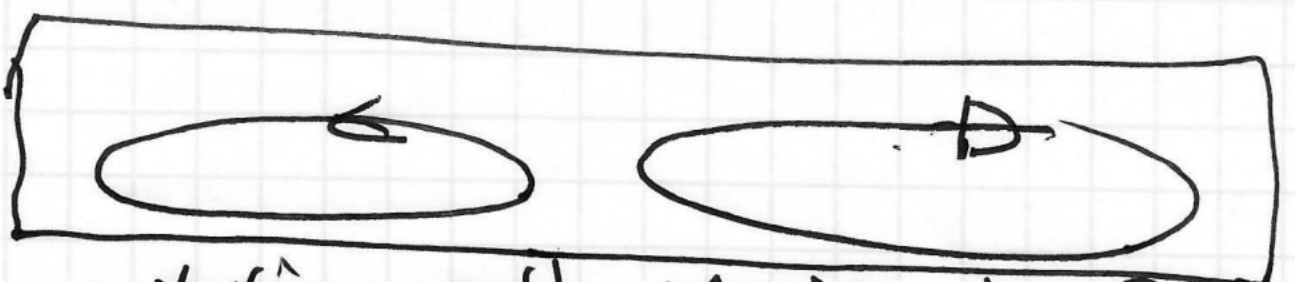


Figure 6: Sketch of final state of fixed-flux convection. Two counter-rotating cells form. Artwork by P.H. Diamond

A Appendix: Cahn-Hilliard equation

In its most familiar form, the Cahn-Hilliard equation may be written

$$\partial_t \psi = D\nabla^2 (\psi^3 - \psi + \epsilon^2 \nabla^2 \psi), \quad (54)$$

where ψ can be understood as a concentration, D a diffusion coefficient, and ϵ a length scale. The quantity in parentheses can be understood as a chemical potential μ . As mentioned

above, this equation describes the dynamics of phase separation. It can be cast in the form of a conservation law

$$\partial_t \psi + \nabla \cdot \mathbf{J} = 0, \quad (55)$$

with the current identified as $\mathbf{J} = -D\nabla\mu$ (à la Fick's law).

The first two terms of μ can be thought of as coming from a free energy functional $F = a(T - T_c)\psi^2/2 + b\psi^4/4$ in the regime $T < T_c$.

References

- [1] P.H. Diamond. Physics 220A lecture notes (2017)
- [2] Y. Pomeau and P. Manneville. “Stability and fluctuations of a spatially periodic convective flow.” *Journal de Physique Lettres* 40 (23), pp. 609–12 (1979)
- [3] P.G. de Gennes. *The Physics of Liquid Crystals*. Clarendon Press (1974)
- [4] M.C. Cross and A.C. Newell. “Convection patterns in large aspect ratio systems.” *Physica D* 10 (3), pp. 299-328 (1984)
- [5] C.J. Chapman and M.R.E. Proctor. “Nonlinear Rayleigh-Bénard convection between poorly conducting boundaries.” *Journal of Fluid Mechanics* 101 (4), pp. 759–82 (1980)
- [6] M. Rieutord. *Fluid Dynamics: An Introduction*. Springer (2015)
- [7] J. W. Cahn and J. E. Hilliard. “Free energy of a nonuniform system. I. Interfacial free energy.” *J. Chem. Phys* 28 (258) (1958)